



# Depletion of atmospheric gaseous elemental mercury by plant uptake at Mt. Changbai, Northeast China

Xuwu Fu<sup>1</sup>, Wei Zhu<sup>1</sup>, Hui Zhang<sup>1</sup>, Jonas Sommar<sup>1</sup>, Ben Yu<sup>1</sup>, Xu Yang<sup>1</sup>, Xun Wang<sup>1,2</sup>, Che-Jen Lin<sup>1,3,4</sup>, and Xinbin Feng<sup>1</sup>

<sup>1</sup>State Key Laboratory of Environmental Geochemistry, Institute of Geochemistry, Chinese Academy of Sciences, 99 Lincheng West Road, Guiyang, 550081, China

<sup>2</sup>University of the Chinese Academy of Sciences, Beijing 100049, China

<sup>3</sup>Department of Civil and Environmental Engineering, Lamar University, Beaumont, Texas 77710, USA

<sup>4</sup>Center for Advances in Water and Air Quality, Lamar University, Beaumont, Texas 77710, USA

Correspondence to: Xinbin Feng (fengxinbin@vip.skleg.cn)

Received: 11 May 2016 – Published in Atmos. Chem. Phys. Discuss.: 1 July 2016

Revised: 2 September 2016 – Accepted: 29 September 2016 – Published: 18 October 2016

**Abstract.** There exists observational evidence that gaseous elemental mercury (GEM) can be readily removed from the atmosphere via chemical oxidation followed by deposition in the polar and sub-polar regions, free troposphere, lower stratosphere, and marine boundary layer under specific environmental conditions. Here we report GEM depletions in a temperate mixed forest at Mt. Changbai, Northeast China. The strong depletions occurred predominantly at night during the leaf-growing season and in the absence of gaseous oxidized mercury (GOM) enrichment ( $GOM < 3 \text{ pg m}^{-3}$ ). Vertical gradients of decreasing GEM concentrations from layers above to under forest canopy suggest in situ loss of GEM to forest canopy at Mt. Changbai. Foliar GEM flux measurements showed that the foliage of two predominant tree species is a net sink of GEM at night, with a mean flux of  $-1.8 \pm 0.3 \text{ ng m}^2 \text{ h}^{-1}$  over *Fraxinus mandshurica* (deciduous tree species) and  $-0.1 \pm 0.2 \text{ ng m}^2 \text{ h}^{-1}$  over *Pinus koraiensis* (evergreen tree species). Daily integrated GEM  $\delta^{202}\text{Hg}$ ,  $\Delta^{199}\text{Hg}$ , and  $\Delta^{200}\text{Hg}$  at Mt. Changbai during 8–18 July 2013 ranged from  $-0.34$  to  $0.91 \text{ ‰}$ , from  $-0.11$  to  $-0.04 \text{ ‰}$  and from  $-0.06$  to  $0.01 \text{ ‰}$ , respectively. A large positive shift in GEM  $\delta^{202}\text{Hg}$  occurred during the strong GEM depletion events, whereas  $\Delta^{199}\text{Hg}$  and  $\Delta^{200}\text{Hg}$  remained essentially unchanged. The observational findings and box model results show that uptake of GEM by forest canopy plays a predominant role in the GEM depletion at Mt. Changbai forest. Such depletion events of GEM are likely to be a widespread phenomenon, suggesting that the forest

ecosystem represents one of the largest sinks ( $\sim 1930 \text{ Mg}$ ) of atmospheric Hg on a global scale.

## 1 Introduction

Mercury (Hg) is a persistent toxic air pollutant that is ubiquitously distributed in the atmosphere. There are three major Hg forms in the atmosphere: gaseous elemental mercury (GEM), particulate bound mercury (PBM), and gaseous oxidized mercury (GOM). The sum of GEM and GOM is known as total gaseous mercury (TGM). Due to its mild reactivity, high volatility, low dry deposition velocity and water solubility, GEM is the most abundant form of Hg in the atmosphere (Gustin and Jaffe, 2010; Holmes et al., 2010). The cycling of GEM in the atmosphere is largely dependent on either direct dry deposition or chemical oxidation followed by wet and dry deposition. The residence time of GEM in the atmosphere is estimated to be from several months to a year, based on the global Hg budget and empirical models (Hedgecock and Pirrone, 2004; Holmes et al., 2006, 2010; Gustin et al., 2015). Over the past decades, our understanding regarding the sources and sinks of atmospheric Hg has been improved (Strode et al., 2007; Selin et al., 2008; Holmes et al., 2010; Amos et al., 2013). For instance, the discovery of atmospheric mercury depletion events (AMDEs) in polar and sub-polar regions demonstrated that atmospheric GEM can be readily removed from the atmosphere via reactive

halogen-induced oxidation, leading to a deposition of up to  $300 \text{ Mg yr}^{-1}$  to the Arctic (Schroeder et al., 1998; Ebinghaus et al., 2002; Lindberg et al., 2002; Steffen et al., 2008). Similar depletion events occurred in the marine boundary layer at middle latitude to a lesser extent (Brunke et al., 2010; Obrist et al., 2011; Timonen et al., 2013). Fast oxidation of GEM by  $\text{O}_3$ , reactive halogens (e.g.,  $\text{BrO}$ ) and  $\text{OH}\cdot$  in the free troposphere has also been observed (Swartzendruber et al., 2006, 2009b; Faïn et al., 2009; Slemr et al., 2009; Lyman and Jaffe, 2012; Shah et al., 2016). These findings indicate that GEM probably has a much shorter atmospheric residence time under specific environmental conditions. Dry deposition of GEM ( $V_d$ ) depends on surface characteristics, meteorological variables, and biological and chemical conditions of soil and water.  $V_d$  over non-vegetated surfaces (e.g., bare soil) and water bodies is typically low (less than  $0.03 \text{ cm s}^{-1}$ ) to counter the emission and re-emission of GEM from these surfaces (Zhang et al., 2009). Therefore soil and water have long been considered a net GEM source (Selin et al., 2007; Holmes et al., 2010). In contrast, strong dry deposition of GEM to vegetated surfaces and wetlands is frequently observed with  $V_d$  up to about  $2 \text{ cm s}^{-1}$  (Zhang et al., 2009), suggesting vegetation is a sink of atmospheric GEM.

Forest represents a dominant terrestrial ecosystem on the Earth and covers an area of  $\sim 4 \times 10^7 \text{ km}^2$ . It readily removes trace gases such as  $\text{CO}_2$ ,  $\text{O}_3$ , sulfur dioxide, nitrogen oxides, and aerosols from the atmosphere (Munger et al., 1996; Finkelstein et al., 2000; Zhang et al., 2001; Pan et al., 2011). However, there are ongoing debates regarding whether or not forest is a sink or a source of atmospheric GEM. Previous laboratory studies suggested that foliar exchange of GEM is bi-directional with net deposition occurring at elevated Hg concentration and net emission under typical background concentrations (Hanson et al., 1995; Erickson and Gustin, 2004; Gustin et al., 2004; Graydon et al., 2006). Lindberg et al. (1998) measured GEM fluxes over a mature deciduous forest using the modified Bowen ratio (MBR) method and suggested that global forest is a net source of GEM with an emission ranging from 850 to  $2000 \text{ Mg yr}^{-1}$ . Later, the observation of Hg fluxes in a deciduous forest using a relaxed eddy accumulation (REA) method showed seasonal shift in flux with a net deposition of GEM during the leaf-growing season (Bash and Miller, 2009). Although the discrepancy in the measured GEM exchanges between forest and atmosphere is partially attributed to the uncertainties of the flux quantification method (Sommar et al., 2013), there is a need to clarify the role of forest ecosystems in the mass budget of atmospheric GEM. A study in Québec, Canada, showed that GEM concentrations at a maple forest site are consistently lower than those measured at an adjacent open site (Poissant et al., 2008). Similarly, the lower GEM concentrations observed in the leaf-growing season at many forest sites across the Atmospheric Mercury Network (AMNet) in USA (Lan et al., 2012) also suggest forest to be a net GEM sink. Currently, it is still un-

clear whether the loss of GEM over forest is caused by direct dry deposition to canopy or chemical conversions of GEM to GOM (Mao et al., 2008).

In this study, we report consistent GEM depletion events during the leaf-growing season (from May to September) in a temperate mixed forest in Northeast China over a timescale of 7 years. Atmospheric Hg speciation, vertical gradient of GEM, foliage–air and soil–air exchange flux of GEM and isotope signatures of GEM samples have also been observed in an intensive campaign to explore the possible mechanisms responsible for the observed GEM depletion.

## 2 Material and methods

### 2.1 Site description

The study site ( $42^\circ 24' 0.1'' \text{ N}$ ,  $128^\circ 06' 25'' \text{ E}$ , 738 m above sea level) is located in a temperate broadleaf and Korean pine mixed forest on the northern slope of Mt. Changbai (Fig. S1 in the Supplement). The forest is dominated by tree species of *Pinus koraiensis*, *Fraxinus mandshurica*, *Tilia amurensis*, *Acer mono* and *Quercus mongolica*. The height of the forest canopy is 5–22 m (mean = 18.3 m) with the heights of mature trees ( $> 50 \text{ yr}$ ) and young trees ( $< 20 \text{ yr}$ ) and shrubs ranging from 15 to 22 m and from 5 to 10 m, respectively. Regions to the east and south of the site consist of pristine forest with little anthropogenic influence (Fu et al., 2012). Most of the regional industrial sources are located more than 50 km west of the sampling site (Fig. S1).

### 2.2 Atmospheric Hg measurements

From October 2008 to July 2013 and from July 2014 to December 2015, TGM concentrations were continuously measured using an automated Hg vapor analyzer (Tekran<sup>®</sup> 2537, Tekran Inc., Canada). The analyzer has been used extensively for atmospheric TGM measurements worldwide. The analyzer was calibrated automatically every 25 h using the internal  $\text{Hg}^0$  permeation source. The permeation rate of the internal source was manually calibrated every 4–6 months by using an external Hg vapor source (Tekran<sup>®</sup> 2505). The sampling inlet was mounted at a height of 24 m above ground level (a.g.l.,  $\sim 3 \text{ m}$  above canopy) by using a 25 m Teflon tube and a 15 m heated Teflon tube. Atmospheric TGM consists of GEM and GOM. Gustin et al. (2013, 2015) proposed that GOM could be transformed to GEM within the uncovered Teflon tubing, which in turn would be transported efficiently through the tubing and quantified by the Tekran analyzer. However, GOM generally constitutes a small portion of TGM (a mean of 0.32 % on the basis of 1 year of measurements, and will not exceed 1 % using a 3-fold correction factor to adjust GOM concentrations measured by the Tekran<sup>®</sup> speciated system) (Gustin et al., 2015). Therefore, we interpret the TGM observations as GEM throughout the paper.

GEM, GOM and PBM were measured using the Tekran<sup>®</sup> 2537/1130/1135 unit (Tekran Inc., Canada) from July 2013 to July 2014. The sampling inlet was positioned at 4 m a.g.l. in a small clearing plot with tall trees of ~5 m from the system. This system has been widely used and described in detail by many earlier studies (Landis et al., 2002; Lindberg et al., 2002; Lan et al., 2012; Fu et al., 2016b). Briefly, GOM, PBM, and GEM in ambient air were collected onto a KCl-coated annular denuder, quartz fiber filter and dual gold cartridges in sequence. This system was programmed to collect GOM and PBM at 1 h intervals at a volumetric flow rate of 10 L min<sup>-1</sup>. GEM was collected from air samples at 5 min intervals at a volumetric flow rate of 1.0 L min<sup>-1</sup>. Once collected, Hg is thermally decomposed from each unit and detected by cold vapor atomic fluorescence spectroscopy (CVAFS) as Hg<sup>0</sup>. A KCl-coated denuder, Teflon-coated glass inlet, and impactor plate were replaced bi-weekly and quartz filters were replaced monthly. Denuders and quartz filters were prepared and cleaned before field sampling following the methods in Tekran technical notes. GEM concentrations measured at 4 m a.g.l. in the small clearing plot and at 45 m a.g.l. (~24 m above canopy) did not bias significantly with each other with a mean difference of 0.03 ng m<sup>-3</sup> (3 % of the mean GEM concentration during the study period) (Fig. S2). The two Tekran instruments used for this comparison were run side by side for 2 days in the laboratory and showed a mean systematic uncertainty of 1.8 ± 1.1 % (ranging from 0 to 5.7 %). This indicates that the measurements at 4 m a.g.l. in the small clearing plot did not significantly underestimate the GEM concentrations of ambient air in the study area. In the study area, GEM also has a fast dry deposition velocity within the forest (more details in sections below), although to a lesser extent compared to atmospheric GOM. We therefore assume that the measurements of GOM in the clearing plot did not result in significantly biased low GOM concentrations and were representative of ambient air in the study area.

Vertical profiles of GEM concentrations at 1, 10, 24, and 45 m a.g.l. within the forest were measured from 10 to 15 July 2013 using the Tekran<sup>®</sup> 2537 analyzer and the Tekran<sup>®</sup> 1115 Synchronized Multi-Port manifold (Tekran Inc., Canada). The sampling duration of GEM during the vertical gradient measurements was programmed to be 2.5 min, and switching of ports of the manifold was made every 5 min.

The GEM detection limit for 7.5 L samples measured with a Tekran<sup>®</sup> 2537 analyzer as specified by Tekran Instrument Corporation is 0.1 ng m<sup>-3</sup>. Due to the lack of understanding of the specific forms and calibration standards of GOM, there are uncertainties regarding the GOM measurements (Gustin et al., 2015). Previous studies suggested that GOM measured by the Tekran system could be biased low and a correction factor of 3 should be applied for adjusting GOM concentrations measured by the Tekran system (Gustin et al., 2013, 2015; Huang et al., 2013; Huang and Gustin, 2015). Tekran<sup>®</sup> 2537's default integration at low Hg loading (~1 pg

per cycle) was reported to have a 25 % underestimation of GEM concentration. This could also underestimate GOM concentrations when GOM concentrations were lower than 2 pg m<sup>-3</sup> (Swartzendruber et al., 2009a). These analytical uncertainties are taken into account for the discussions of the GEM depletion mechanism in the Results and Discussion section.

### 2.3 Foliar GEM exchange

Exchange flux of GEM between leaf and atmosphere was measured using a new dynamic flux bag method described by Graydon et al. (2006) which is thought to maintain the normal physiological function of enclosed foliage. Briefly, a Tedlar<sup>®</sup> gas sampling bag (~20 L volume, polyvinyl fluoride, DuPont, USA) enclosed living intact leaves, and the foliar GEM flux was obtained by measuring the difference in GEM concentrations at the inlet and outlet of the flux bag. Ambient air was pumped into the flux bag using a Mini Diaphragm vacuum pump (N89 KTDC, KNF, Germany, oil-free, brushless and with a diaphragm coated with PTFE). GEM flux was calculated using Eq. (1):

$$F = (C_o - C_i) \times Q/A, \quad (1)$$

where  $F$  is the foliar GEM flux in ng m<sup>-2</sup> h<sup>-1</sup>, with positive and negative values representing emission and deposition, respectively,  $C_o$  and  $C_i$  are the GEM concentrations at the outlet and inlet of the flux bag, respectively, which were measured by the Tekran<sup>®</sup> 2537 analyzer,  $Q$  is the flushing flow rate of air through the flux bag (0.5 m<sup>3</sup> h<sup>-1</sup>), and  $A$  is the single-sided leaf area enclosed by the flux bag in m<sup>2</sup>.

Two tree species, *Fraxinus mandshurica* (deciduous tree species) and *Pinus Koraiensis* (evergreen tree species), were selected for the foliar GEM flux measurement. They are the predominant species in the study area with the basal coverage of the *Fraxinus Mandschurica* and *Pinus Koraiensis* accounting for 26.3 and 27.5 % of the total basal area (Dai et al., 2011). Both selected species for flux measurement are mature with a height of ~20 m. The flux bag was installed at a height of 15 m a.g.l. Foliar GEM fluxes over *Fraxinus mandshurica* and *Pinus Koraiensis* were continuously measured during 16–17 and 17–18 July 2013, respectively, and 24 h continuous flux data were obtained for each species. The mean blank of the flux chamber measured before and after the field experiment was  $-0.02 \pm 0.04$  ng m<sup>-2</sup> h<sup>-1</sup> ( $n = 24$ ), which was indistinguishable from zero and not used to calibrate the measured fluxes.

### 2.4 Isotopic composition of atmospheric GEM

From 8 to 18 July 2013, GEM samples were collected at 4 m a.g.l. at the study site for Hg isotope analysis using a chlorine-impregnated activated carbon (CLC) trap (Fu et al., 2014). Atmospheric GEM was collected daily (24 h sampling duration) at a flow rate of 10 L min<sup>-1</sup>. CLC traps collect

GEM at > 95 % efficiency at the given sampling flow rate (Fu et al., 2014). To remove air particles, a 47 mm diameter Teflon filter (pore size 0.2  $\mu\text{m}$ ) was installed at the inlet of the CLC trap. The CLC trap was kept warm (50–70 °C) during sampling using silicone rubber heating pads (RadioSpares) to prevent water condensation. The sampling flow rate of CLC traps was regulated via a gas flow meter installed at the outlet of the vacuum pump, and the total sampling volumes of the CLC traps were recorded using a gas meter, calibrated to standard volumes under a standard pressure of 1013 hPa and a standard temperature of 273.14 K using a Bios Defender.

After the completion of field sampling, CLC traps were sealed with silicone stoppers and three successive polyethylene bags and stored in a clean environment until pre-concentration into trap solutions for Hg isotope analysis. GEM collected by CLC traps was pre-concentrated into a reverse aqua regia solution ( $v/v$ , 2HNO<sub>3</sub>/1HCl) in the laboratory using a double-stage combustion protocol for Hg isotope analysis (Biswas et al., 2008; Sun et al., 2013; Fu et al., 2014). Hg isotope ratios were determined by Nu-Plasma MC-ICP-MS following a previously established method (Yin et al., 2013). Hg isotopic composition is reported in delta notation ( $\delta$ ) in per mil referenced to the bracketed NIST 3133 Hg standard (Blum and Bergquist, 2007):

$$\delta^{xxx}\text{Hg} = \left( \frac{\left( \frac{xxx\text{Hg}}{198\text{Hg}} \right)_{\text{sample}}}{\left( \frac{xxx\text{Hg}}{198\text{Hg}} \right)_{\text{SRM3133}}} - 1 \right) \times 1000 \text{‰} \quad (2)$$

Mass-independent fractionation (MIF) values are expressed by “capital delta ( $\Delta$ )” notation (‰), which is the difference between the measured values of  $\delta^{199}\text{Hg}$ ,  $\delta^{200}\text{Hg}$ ,  $\delta^{201}\text{Hg}$  and those predicted from  $\delta^{202}\text{Hg}$  using the kinetic MDF law (Blum and Bergquist, 2007):

$$\Delta^{199}\text{Hg}(\text{‰}) = \delta^{199}\text{Hg} - (0.252 \times \delta^{202}\text{Hg}), \quad (3)$$

$$\Delta^{200}\text{Hg}(\text{‰}) = \delta^{200}\text{Hg} - (0.502 \times \delta^{202}\text{Hg}), \quad (4)$$

$$\Delta^{201}\text{Hg}(\text{‰}) = \delta^{201}\text{Hg} - (0.752 \times \delta^{202}\text{Hg}). \quad (5)$$

The analytical uncertainty of isotopic analysis was obtained by repeated analysis of the UM-Almaden standard. The overall mean values of  $\delta^{202}\text{Hg}$  and  $\Delta^{199}\text{Hg}$  for all the UM-Almaden standards were  $-0.57 \pm 0.09 \text{‰}$  and  $-0.03 \pm 0.04 \text{‰}$  (2 SD,  $n = 12$ ), respectively, consistent with previously reported values (Blum and Bergquist, 2007). In the present study, the analytical uncertainty of CV-MC-ICPMS isotope analysis is the 2 SD uncertainty of the UM-Almaden standard, unless the 2 SD uncertainty on repeated analysis of the same sample over different analytical sessions is larger.

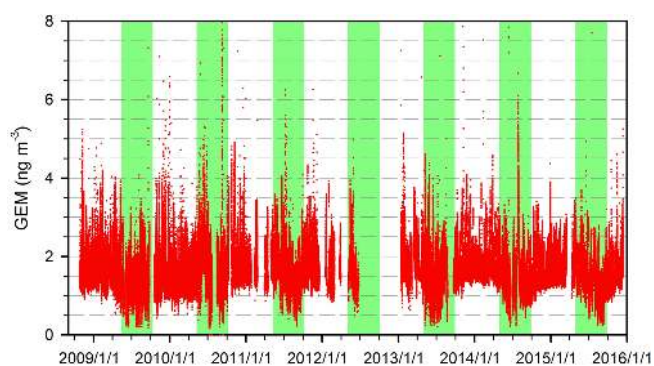


**Figure 1.** Atmospheric 5 min GEM concentrations at Mt. Changbai from October 2008 to December 2015 (the leaf-growing season is marked as the shaded area).

### 3 Results and discussion

#### 3.1 Characteristics of depletion events at Mt. Changbai

From October 2008 to December 2015, we observed 52 strong depletion events with dips of GEM concentrations < 0.5  $\text{ng m}^{-3}$ . These depletions occurred predominantly at night during the leaf-growing season and generally lasted for 0.5–6 h (Fig. 1). GEM concentrations during the strong depletion events decreased rapidly from a background level of  $\sim 1.50 \text{ ng m}^{-3}$  around noon to < 0.5  $\text{ng m}^{-3}$  at night, corresponding to > 65 % loss of GEM. It is worth noting that depletions also occurred at night during the non-leaf-growing season (January–April and October–December). However, depletions of atmospheric GEM during the non-leaf-growing season were less pronounced and frequent compared to the leaf-growing season, with dips of GEM concentrations generally higher than 1.0  $\text{ng m}^{-3}$ , which represented 2/3 of the background level at the study site (Fig. 1). Figure 2 shows the representative depletion events in the summers of 2010 and 2013. Strong depletion of GEM consistently occurred at night. During the 7–13 July 2010 period, a nearly complete depletion occurred with GEM concentrations decreasing from 1.6–2.0  $\text{ng m}^{-3}$  at noon to nearly zero at night (removal of GEM averaged  $1.83 \pm 0.35 \text{ ng m}^{-3}$  ( $n = 7$ )). The daytime peak GEM concentrations for the depletion events during 9–23 July 2013 ranged from 1.50 to 2.31  $\text{ng m}^{-3}$ , and the lowest GEM concentrations at night were 0.35–0.99  $\text{ng m}^{-3}$ , yielding an averaged removal of GEM of  $1.08 \pm 0.23 \text{ ng m}^{-3}$  ( $n = 12$ ).

GEM concentrations during the strong nighttime atmospheric GEM depletion events ( $n = 10$ , defined as nighttime dips in GEM concentrations < 0.5  $\text{ng m}^{-3}$ ) from July 2013 to July 2014 were typically low (< 3  $\text{pg m}^{-3}$  with a mean value of 0.8  $\text{pg m}^{-3}$ ). This is in contrast to previously characterized GEM depletions in the polar and sub-polar regions, marine boundary layer and free troposphere where depletions of GEM were accompanied by strong GEM enhancements (up

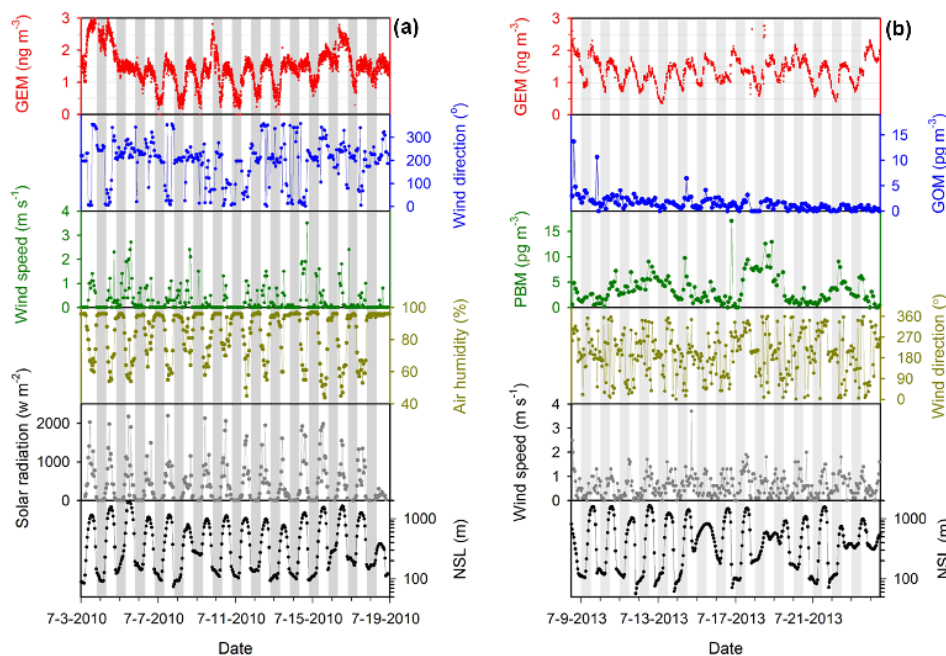


**Figure 2.** Time series of (a) GEM (5 min mean) and meteorological parameters from 3 to 19 July 2010 and (b) speciated atmospheric Hg (GEM, GOM, and PBM) and meteorological parameters from 8 to 24 July 2013 (nighttime is marked as the shaded area).

to 195–1200  $\text{pg m}^{-3}$ ) (Lindberg et al., 2002; Swartzendruber et al., 2006; Sheu et al., 2010; Obrist et al., 2011; Lyman and Jaffe, 2012). Wind speed was low (mean of  $0.1 \text{ m s}^{-1}$  during 7–13 July 2010 and  $0.4 \text{ m s}^{-1}$  during 9–23 July 2013) during the nighttime depletion events at the study site (Fig. 2). A shallow nocturnal boundary layer (NBL; see text in the Supplement) was frequently developed when the depletion occurred with a mean height of 146 m (74–200 m) during 7–13 July 2010 and 209 m (57–300 m) during 9–23 July 2013 (Fig. 2). The low winds and shallow NBL limited the transport of air masses at the sampling site and facilitated a continuous depletion of GEM in the presence of vegetative uptake of GEM (more details in the sections below). During daytime, the surface wind speed and NBL depth increased due to solar heating (Talbot et al., 2005), enabling the downward transport of GEM from upper air, resulting in the increasing GEM concentrations.

Strong depletion of GEM during summer nighttime has also been observed at forest sites in North America (e.g., St. Anicet Maple forest station in Canada, and Piney Reservoir, Huntington Wildlife, Thompson Farm, Kejimikujik National Park, and Stilwell in AMNet, USA) (Mao et al., 2008; Poissant et al., 2008; Lan et al., 2012). Such depletion of GEM in forest ecosystems is likely a widespread phenomenon globally. The depletion at forest sites was different from the atmospheric mercury depletion events (AMDEs) elsewhere. For instance, the AMDEs at Cape Point, coast of South Africa, and the Dead Sea, Israel, are mostly observed during daytime (Brunke et al., 2010; Obrist et al., 2011). The AMDEs in the

polar regions occur exclusively during polar sunrise in spring and do not exhibit a well-defined diurnal pattern (Schroeder et al., 1998; Ebinghaus et al., 2002; Lindberg et al., 2002).

### 3.2 Vertical gradient of GEM observed at Mt. Changbai

A clear vertical gradient of GEM concentrations was observed at the study site, with increasing GEM concentrations with respect to sampling altitude (Fig. 3). The average difference in GEM concentrations between 45 and 1 m (all in a.g.l.,  $\Delta\text{GEM}_{45-1\text{m}}$ ) was  $0.22 \pm 0.15 \text{ ng m}^{-3}$  ( $n = 330$ ),  $\sim 20\%$  of the mean GEM concentration at 45 m a.g.l. Average differences in GEM concentrations between 45 and 24 m ( $\Delta\text{GEM}_{45-24\text{m}}$ ), between 24 and 10 m ( $\Delta\text{GEM}_{24-10\text{m}}$ ), and between 10 and 1 m ( $\Delta\text{GEM}_{10-1\text{m}}$ ) were  $0.11 \pm 0.10$ ,  $0.05 \pm 0.09$ , and  $0.06 \pm 0.11 \text{ ng m}^{-3}$  ( $n = 330$ ), respectively. The observed gradient suggested that the forest at the study site is a net sink for atmospheric GEM, in contrast to the vertical GEM gradients observed in a mature hardwood forest (between 30 and 40 m a.g.l.) in Walker Branch Watershed, Tennessee, USA, during daytime, which showed decreasing GEM concentrations with sampling altitude above the forest canopy (Lindberg et al., 1998). This difference might be caused by the different forest structure and elevated emission flux of GEM from forest soil ( $7.5 \text{ ng m}^{-2} \text{ h}^{-1}$  in Walker Branch Watershed vs.  $2.8 \text{ ng m}^{-2} \text{ h}^{-1}$  at Mt. Changbai, Fig. S3) in Walker Branch Watershed (Kim et al., 1995; Lindberg et al., 1998).

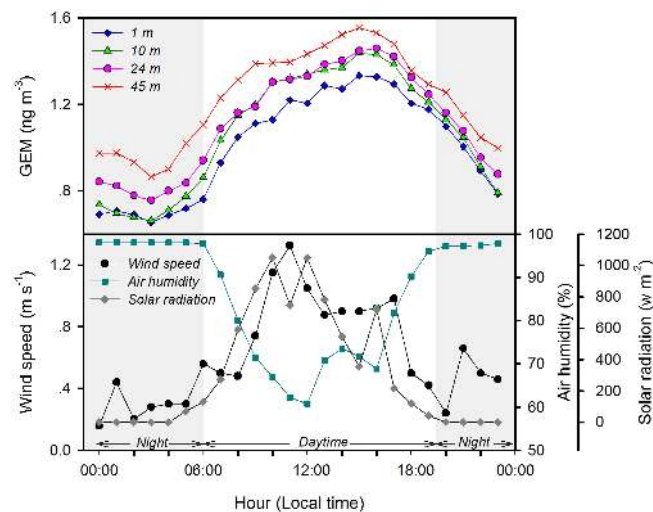


**Figure 3.** Diurnal variations of GEM concentrations at different height and meteorological parameters in Mt. Changbai forest from 10 to 15 July 2013 (nighttime is marked as the shaded area).

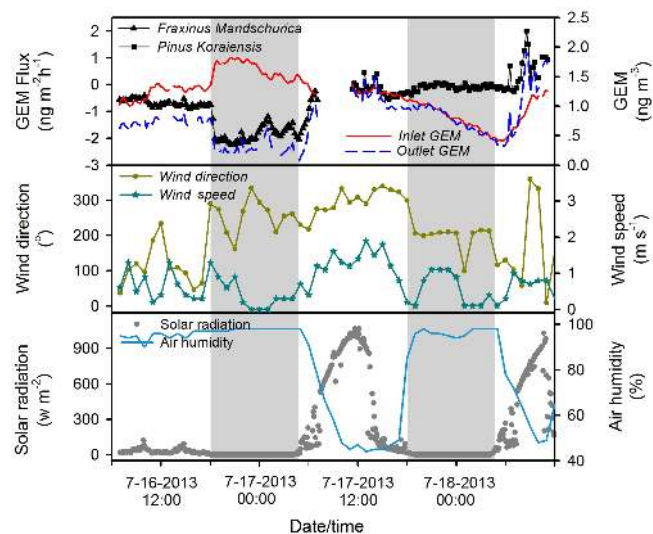


**Figure 4.** Foliar Hg flux over *Fraxinus Mandschurica* and *Pinus Koraiensis*, inlet and outlet GEM concentrations from flux bag and meteorological parameters at Mt. Changbai in July 2013 (nighttime is marked as the shaded area).

The vertical gradients of GEM at Mt. Changbai showed clear diurnal trends (Figs. 3 and S4).  $\Delta\text{GEM}_{45-24\text{m}}$  and  $\Delta\text{GEM}_{24-10\text{m}}$  values were comparably higher at night (means of 0.13 and 0.08  $\text{ng m}^{-3}$ , respectively) than those during daytime (means of 0.09 and 0.02  $\text{ng m}^{-3}$ , respectively). The smaller daytime  $\Delta\text{GEM}_{45-24\text{m}}$  and  $\Delta\text{GEM}_{24-10\text{m}}$  were a result of weaker dry deposition of GEM to the forest canopy (more discussion later). A strong negative correlation between the  $\Delta\text{GEM}_{24-10\text{m}}$  and wind speed ( $r^2 = 0.55$ ,  $p < 0.01$ ) also suggested stronger vertical mixing during daytime inhibited the buildup of GEM gradi-

ent. The diurnal trend of  $\Delta\text{GEM}_{10-1\text{m}}$  was opposite to  $\Delta\text{GEM}_{45-24\text{m}}$  and  $\Delta\text{GEM}_{24-10\text{m}}$ , with larger values during daytime (mean = 0.09  $\text{ng m}^{-3}$ ) and lower values at night (mean = 0.04  $\text{ng m}^{-3}$ ).

### 3.3 Foliage–air exchange flux of GEM

Mean foliar GEM fluxes over *Fraxinus Mandschurica* and *Pinus Koraiensis* were  $-1.2 \pm 0.6$  ( $-2.2$  to  $-0.2 \text{ ng m}^{-2} \text{ h}^{-1}$ ) and  $0.0 \pm 0.4 \text{ ng m}^{-2} \text{ h}^{-1}$  ( $-0.5$  to  $2.0 \text{ ng m}^{-2} \text{ h}^{-1}$ ), respectively (Fig. 4). Mean ambient GEM concentrations during the flux measurements over *Fraxinus Mandschurica* and *Pinus Koraiensis* were  $1.42 \pm 0.23$  and  $0.93 \pm 0.28 \text{ ng m}^{-3}$ , respectively, below the background concentrations of GEM in the Northern Hemisphere ( $1.5\text{--}1.7 \text{ ng m}^{-3}$ ) (Lindberg et al., 2007). The low GEM deposition flux over *Pinus Koraiensis* was partially attributed to the low ambient GEM concentration that weakens the deposition flux (Hanson et al., 1995; Ericksen and Gustin, 2004). The mean deposition fluxes over *Fraxinus Mandschurica* ( $0.7 \pm 0.1 \text{ ng m}^{-2} \text{ h}^{-1}$ ) was much greater than that over *Pinus Koraiensis* ( $0.0 \pm 0.5 \text{ ng m}^{-2} \text{ h}^{-1}$ ) given the same GEM ( $1.0\text{--}1.4 \text{ ng m}^{-3}$ ) range (Fig. 4), suggesting that GEM deposition flux varies with tree species, with deciduous tree species inducing higher deposition compared to evergreen tree species (Millhollen et al., 2006).

The observed foliar GEM fluxes over *Fraxinus Mandschurica* and *Pinus Koraiensis* were within the range of reported values (means =  $-6$  to  $3.5 \text{ ng m}^{-2} \text{ h}^{-1}$ ) (Ericksen et al., 2003; Frescholtz and Gustin, 2004; Gustin et al., 2004; Graydon et al., 2006; Poissant et al., 2008; Stamenkovic and Gustin, 2009). A diurnal pattern with higher deposition fluxes at night was observed for both species. The higher deposition flux at night can be attributed to enhanced foliar GEM uptakes. As seen in Fig. 4, differences in GEM concentrations between the inlet and outlet streams of the flux bag (corresponding to the net loss of atmospheric GEM to foliage) over *Fraxinus Mandschurica* at night (mean =  $1.31 \pm 0.23 \text{ ng m}^{-3}$ ) were much higher compared to daytime (mean =  $0.48 \pm 0.11 \text{ ng m}^{-3}$ ). It has been suggested that lower  $\text{O}_3$  and higher relative humidity (RH) could facilitate the uptake of GEM by foliage (Lindberg and Stratton, 1998; Stamenkovic and Gustin, 2009).  $\text{O}_3$  and RH at the study site showed strong diurnal patterns with decreasing  $\text{O}_3$  concentrations and increasing RH at night (Fig. S5), which may explain the higher deposition fluxes of GEM to foliage at night. Both stomatal and non-stomatal uptakes have been suggested to be responsible for the observed foliage–atmosphere GEM exchange (Zhang et al., 2005; Stamenkovic and Gustin, 2009). Stamenkovic and Gustin (2009) found that GEM deposition flux to foliage remained essentially unchanged whether or not stomata are open. This indicates that the non-stomatal route plays an important role in the uptake of GEM by foliage, consistent with the observations in this study. Previous studies suggested that foliar ex-

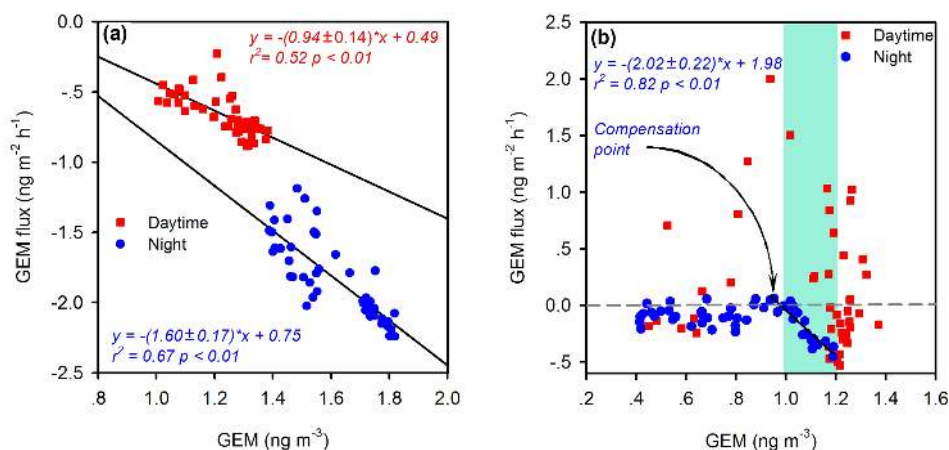


**Figure 5.** Daytime and nighttime correlations between atmospheric GEM concentrations and foliar GEM fluxes over (a) *Fraxinus Mandschurica* and (b) *Pinus Koraiensis*.

change of GEM is bi-directional with foliage emitting GEM at global background air GEM concentrations (Hanson et al., 1995; Ericksen and Gustin, 2004; Graydon et al., 2006). With the GEM concentrations in the range of 0.41–1.82  $\text{ng m}^{-3}$  during this study, however, net deposition was observed except for *Pinus Koraiensis* during daytime, when stomata are open. Net emission of GEM from *Pinus Koraiensis* during daytime could be attributed to the enhanced photochemical reduction and re-emission of previously deposited Hg (GEM, GOM and PBM), Hg in dew water and transpiration stream as well as transpiration of  $\text{Hg}^0$  in soil pores (Bishop et al., 1998; Lindberg et al., 1998; Ericksen and Gustin, 2004; Stamenkovic and Gustin, 2009).

The observed foliar GEM fluxes over *Fraxinus Mandschurica* were negatively correlated with the GEM concentrations in the inlet air (Fig. 5a), yielding a compensation point of 0.52  $\text{ng m}^{-3}$  during daytime and 0.47  $\text{ng m}^{-3}$  during nighttime, respectively. No clear correlation between foliar GEM fluxes and ambient GEM concentrations was observed for *Pinus Koraiensis* during daytime. However, a significant negative correlation was observed at night when ambient GEM concentrations were higher than 0.98  $\text{ng m}^{-3}$  (Fig. 5b), which was likely the compensation point for *Pinus Koraiensis* during nighttime. These observed compensation points were comparatively lower than the values (2–3  $\text{ng m}^{-3}$ ) measured in laboratory studies (Ericksen and Gustin, 2004; Graydon et al., 2006), but consistent with the field observation at St. Anicet maple forest, Canada (0.53  $\text{ng m}^{-3}$ ) (Poissant et al., 2008). For *Pinus Koraiensis*, the observed foliar GEM fluxes were not significantly different from zero (mean =  $-0.1 \pm 0.1 \text{ ng m}^{-2} \text{ h}^{-1}$ ) at GEM concentrations lower than the compensation point (0.98  $\text{ng m}^{-3}$ ). A similar conclusion cannot be reached for *Fraxinus Mandschurica* because the ambient GEM concentrations were higher than the respective compensation points during the entire campaign (Fig. 5a). This finding is differ-

ent from previous results that showed net GEM emissions from foliage at ambient GEM concentrations below the compensation points (Hanson et al., 1995; Graydon et al., 2006; Poissant et al., 2008). Based on the field findings, it is likely that the uptake and emission of GEM over the foliage of *Pinus Koraiensis* reached equilibrium during nighttime when the ambient GEM concentrations were below the compensation point.

The total deposition flux of GEM to forest canopy at Mt. Changbai was estimated using Eq. (6):

$$F = \text{LAI} \times \sum_i^n (F_i \times A_i), \quad (6)$$

where  $F$  is the total deposition flux of GEM in  $\text{ng m}^{-2} \text{ h}^{-1}$ , LAI is the mean leaf area index (dimensionless),  $F_i$  is the foliar GEM flux of a tree species ( $i$ ) in  $\text{ng m}^{-2} \text{ h}^{-1}$ , and  $A_i$  is the relative basal area of a tree species ( $i$ ) in percentile (Dai et al., 2011). In this study, it is assumed that the measured mean foliar GEM fluxes over *Fraxinus Mandschurica* and *Pinus Koraiensis* are representative of deciduous tree species and evergreen tree species, respectively. The measured mean LAI at Mt. Changbai during the leaf-growing season was 5.4.

The total deposition fluxes of GEM to forest canopy at Mt. Changbai during nighttime and daytime are estimated to be 7.3 ( $V_d$  of 0.14  $\text{cm s}^{-1}$ ) and 2.5  $\text{ng m}^{-2} \text{ h}^{-1}$  ( $V_d$  of 0.04  $\text{cm s}^{-1}$ ). We acknowledge that, due to the relatively short field sampling periods for the two selected tree species and the fact that foliar GEM flux may vary with tree species, GEM concentrations and other environmental variables, our estimates may have large uncertainties. Nevertheless, the estimates are generally consistent with the measured deposition flux using Hg accumulated in foliage over time. The mean mass-weighted Hg concentration in litter samples at the study site was  $43.0 \pm 29.5 \text{ ng g}^{-1}$  (Table S1 in the Supplement). With the annual litterfall of 486  $\text{g m}^{-2}$  at the site (Zhou et al., 2014), the Hg deposition flux in litterfall was  $20.9 \pm 14.3 \text{ } \mu\text{g m}^{-2} \text{ yr}^{-1}$ . Assuming that the plant foliage had

a constant uptake rate of Hg in the leaf-growing season, the hourly deposition flux of Hg that ends up being contained in litterfall would be  $5.7 \text{ ng m}^{-2} \text{ h}^{-1}$ , comparable to the GEM deposition flux calculated from flux bag observations (daily mean:  $4.9 \text{ ng m}^{-2} \text{ h}^{-1}$ ).

### 3.4 Mechanisms for the observed GEM depletion

Oxidation of GEM by reactive halogens and  $\text{O}_3$  has been proposed to be an important mechanism for GEM depletions observed elsewhere as evidenced by the elevated GOM concentrations (up to  $500\text{--}1200 \text{ pg m}^{-3}$ ) associated with the GEM depletion events and an inverse correlation between GOM and GEM concentrations (Lindberg et al., 2002; Obrist et al., 2011; Lyman and Jaffe, 2012). Based on modeling assessments, the nighttime loss of GEM in forest areas has been suggested to be caused by dry deposition and chemical oxidation (by  $\text{O}_3$ ,  $\text{OH}\cdot$  and  $\text{NO}_3$ ) (Mao et al., 2008). However, the GOM concentrations observed during strong nighttime GEM depletion events at Mt. Changbai were extremely low ( $< 3 \text{ pg m}^{-3}$  with a mean value of  $0.8 \text{ pg m}^{-3}$ ), similar to those observed at other forest sites (Piney Reservoir, Huntington Wildlife, Thompson Farm, Kejimikujik National Park, and Stilwell) in North America (means =  $0.5\text{--}4 \text{ pg m}^{-3}$  at summertime night) (Lan et al., 2012). In addition, concentrations of many atmospheric oxidants (e.g.,  $\text{O}_3$ ,  $\text{OH}\cdot$ ,  $\text{NO}_3$ ,  $\text{BrO}$ ) at global forest sites were low (Spivakovsky et al., 2000; Yang et al., 2005; Rinne et al., 2012; Hens et al., 2014), which does not support significant conversion of GEM to GOM. Given the environmental condition at Mt. Changbai, the dry deposition flux of GOM was estimated to be  $0.034 \text{ ng m}^{-2} \text{ h}^{-1}$ , using the mean nighttime GOM concentration ( $0.8 \text{ pg m}^{-3}$ ) measured during the strong GEM depletion events and reported  $V_d$  of GOM ( $0.1$  to  $5.9 \text{ cm s}^{-1}$  with a mean of  $1.2 \text{ cm s}^{-1}$ ) to forest canopy (Lindberg and Stratton, 1998; Rea et al., 2000; Zhang et al., 2012). Even with a correction factor of 3 to account for the potential underestimation of GOM concentration by the Tekran<sup>®</sup> speciation system (Gustin et al., 2013, 2015; Huang et al., 2013), the deposition flux contributed by GOM is  $0.1 \text{ ng m}^{-2} \text{ h}^{-1}$ . Assuming that all GOM was formed through in situ oxidation of GEM, the chemical pathway would contribute merely 1.4% of the measured deposition flux of GEM to forest canopy during the nighttime depletion events.

Measurements of GEM isotopic composition also provided insight into the mechanisms responsible for the GEM depletion at Mt. Changbai.  $\delta^{202}\text{Hg}$ ,  $\Delta^{199}\text{Hg}$ , and  $\Delta^{200}\text{Hg}$  of the daily GEM samples from 8 to 18 July 2013 were  $-0.34$  to  $0.91\text{‰}$ ,  $-0.11$  to  $-0.04\text{‰}$  and  $-0.06$  to  $0.01\text{‰}$ , respectively ( $n = 10$ , Fig. 6, Table S2). These are consistent with the observations in the Great Lakes region, Barrow, Alaska, Pensacola, Florida, and Wisconsin forest in the USA and the Pic du Midi Observatory in France ( $\delta^{202}\text{Hg}_{\text{GEM}} = -0.12$  to  $1.43\text{‰}$ ,  $\Delta^{199}\text{Hg}_{\text{GEM}} = -0.31$  to  $-0.01\text{‰}$ ,  $\Delta^{200}\text{Hg} = -0.11$  to  $0.1\text{‰}$ ) (Gratz et al., 2010;

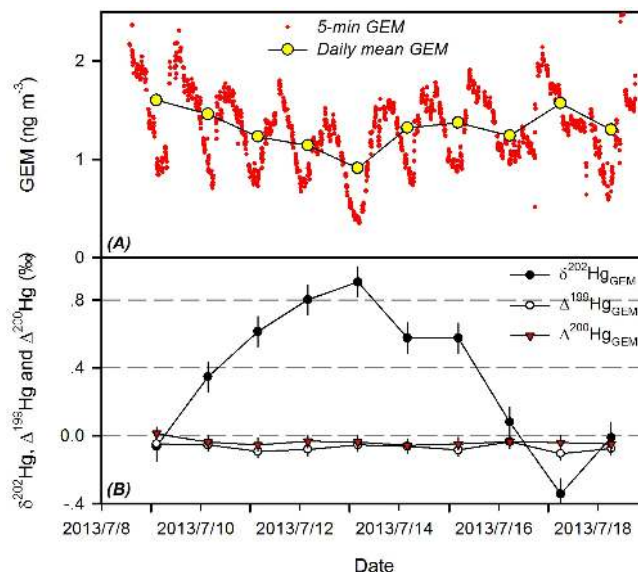


**Figure 6.** Temporal variation in (a) atmospheric GEM concentrations and (b)  $\delta^{202}\text{Hg}$ ,  $\Delta^{199}\text{Hg}$  and  $\Delta^{200}\text{Hg}$  values of daily integrated atmospheric GEM from 9 to 18 July 2013.

Sherman et al., 2010; Demers et al., 2013, 2015; Fu et al., 2016a). A large positive  $\delta^{202}\text{Hg}_{\text{GEM}}$  shift was associated with strong GEM depletions, whereas  $\Delta^{199}\text{Hg}_{\text{GEM}}$  and  $\Delta^{200}\text{Hg}_{\text{GEM}}$  remained unchanged. The  $\delta^{202}\text{Hg}_{\text{GEM}}$  was up to  $0.91\text{‰}$  during the most pronounced depletion event (on 13 July 2013, daily mean GEM of  $0.91 \text{ ng m}^{-3}$ ),  $1.05\text{‰}$  higher than the values at the beginning and end of the sampling period (on 9 and 17 July 2013, mean GEM =  $1.57\text{--}1.60 \text{ ng m}^{-3}$ , mean  $\delta^{202}\text{Hg}_{\text{GEM}} = -0.14\text{‰}$ ). The  $\delta^{202}\text{Hg}_{\text{GEM}}$  values were anti-correlated with GEM concentrations ( $r^2 = 0.58$ ,  $p < 0.01$ ), whereas no clear relationship can be established between  $\Delta^{199}\text{Hg}$  and  $\Delta^{200}\text{Hg}_{\text{GEM}}$  values and atmospheric GEM concentrations ( $p$  values for both  $> 0.05$ ). The lower  $\delta^{202}\text{Hg}_{\text{GEM}}$  values at the beginning and end of the sampling period were likely representative of the regional background  $\delta^{202}\text{Hg}_{\text{GEM}}$  signatures as the mean GEM concentrations of the two samples ( $1.46\text{--}1.60 \text{ ng m}^{-3}$ , Table S2) were close to the long-term GEM mean concentration at Mt. Changbai, whereas the positive  $\delta^{202}\text{Hg}_{\text{GEM}}$  shifts during 11–15 July 2013 were most likely due to the uptake of GEM by forest foliage, which has been known to induce mass-dependent fractionation (MDF,  $\delta^{202}\text{Hg}$  signature) and negligible MIF ( $\Delta^{199}\text{Hg}$ ,  $\Delta^{200}\text{Hg}$  signatures) of Hg isotopes (Demers et al., 2013; Enrico et al., 2016). MDF and MIF of Hg isotopes caused by GEM oxidation have not been well characterized. Studies observed both significant MDF and MIF of Hg isotopes during aqueous- and gas-phase chemical oxidation of elemental Hg (Stathopoulos, 2014; Sun et al., 2016). Our study at Pic du Midi, France (2877 m above sea level), also observed clear shifts in  $\delta^{202}\text{Hg}_{\text{GEM}}$  and  $\Delta^{199}\text{Hg}_{\text{GEM}}$  during oxidation of GEM to GOM, indicating



both MDF and MIF could occur during “net oxidation” of GEM in the ambient air (Sonke et al., 2016). Therefore, we conclude that foliar uptake of GEM played a predominant role in the GEM depletion at Mt. Changbai.

To answer the question whether or not GEM dry deposition to forest canopy alone can explain the GEM depletion at Mt. Changbai, the forced change of GEM concentrations by canopy uptake at the sampling height of 24 m a.g.l. under a typical NBL height of 100 m was simulated using a box model (see text in the Supplement). The box model results suggest that complete GEM depletions can be achieved by canopy uptake alone in the presence of shallow NBL and low vertical turbulent diffusivity (Fig. 7). With a dry deposition GEM flux of  $7.3 \text{ ng m}^{-2} \text{ h}^{-1}$  (Sect. 3.3) and turbulent diffusivity of  $0.1\text{--}1.0 \text{ cm s}^{-1}$  at night (Fig. S6), the model predicted that GEM concentrations can be decreased to nearly  $0 \text{ ng m}^{-3}$  (Fig. 7). Depletion cannot occur during daytime, mainly due to the low dry deposition flux ( $\sim 2.5 \text{ ng m}^{-2} \text{ h}^{-1}$ ), high vertical turbulent diffusivity ( $1\text{--}100 \text{ cm s}^{-1}$ ) and absence of a shallow NBL (Fig. 7 and Fig. S6 in the Supplement). The GEM depletion event at Mt. Changbai showed a clear seasonal trend, with the depletion occurring more frequently and pronouncedly during the leaf-growing season (Fig. 1). This can be attributed to (1) seasonal LAI changes (Fig. S7a), (2) lower wind speed during the leaf-growing season (Fig. S7b), and (3) the wind direction that inhibited the transport of polluted air from anthropogenic source regions ( $90\text{--}202^\circ$ , natural preserve areas without significant local and regional sources) during the leaf-growing season (Fig. S7c). LAI is much higher during the leaf-growing season compared to the non-leaf-growing season ( $< 2$ , Fig. S7a) (Shi et al., 2008). Higher LAI values indicate higher dry deposition fluxes of GEM to forest canopy. The low wind speed facilitated the buildup of a shallow NBL.

#### 4 Conclusions and implications for the global atmospheric Hg cycling

Strong depletions of atmospheric GEM were consistently observed during the leaf-growing season in Mt. Changbai forest, Northeast China. The depletions occurred exclusively at night in the absence of GEM enrichments. This is in contrast to previously characterized GEM depletions in the polar and sub-polar regions, marine boundary layer and free troposphere where depletions of GEM were mainly caused by fast chemical oxidation of GEM to GOM followed by deposition. The measurements of GEM vertical gradients, foliar GEM fluxes, atmospheric speciated Hg and ambient GEM isotope compositions suggest foliar uptake of GEM played a predominant role in the GEM depletion at Mt. Changbai.

Forests cover  $\sim 30\%$  ( $\sim 40$  million  $\text{km}^2$ ) of the Earth's land surface. There is a need to quantitatively assess the role of global forest in global Hg cycling. Tables S3, S4, and

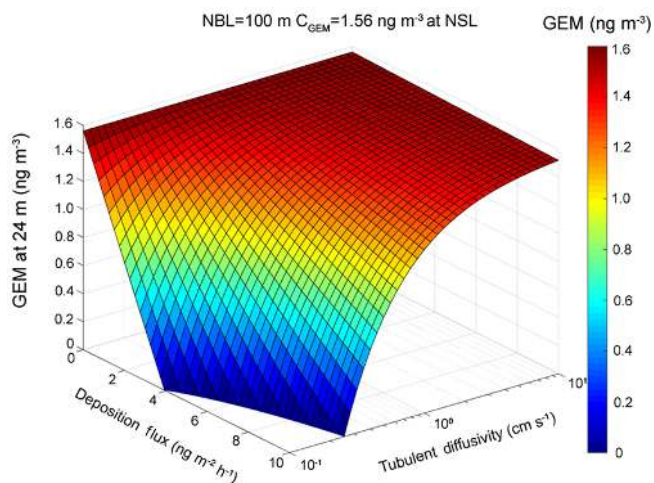


**Figure 7.** Modeling predicted variations of GEM concentration at the height of 24 m a.g.l. with dry position fluxes of GEM to forest canopy and vertical turbulent diffusivity under a typical NBL height of 100 m and background GEM concentration of  $1.56 \text{ ng m}^{-3}$ .

S5 summarize the published data of litterfall fluxes at 68 forest sites, throughfall fluxes at 23 forest sites, and emissions from forest floors at 31 forest sites in North America, Europe, Asia, and South America. For the regions (Africa and Oceania) that lack observational data, it is assumed that the median values of the published data are representative. There have not been reliable data on Hg emission from forest canopies via evapotranspiration. We therefore use the observed xylem Hg concentrations and total evapotranspiration from the global forests to estimate Hg emissions from this sector (Bishop et al., 1998; Baldocchi and Ryu, 2011).

Using a mass balance approach, we estimated that global inputs of Hg via litterfall and throughfall were  $1232$  and  $1338 \text{ Mg yr}^{-1}$ , respectively. Hg emissions via the evasion from soil and plant evapotranspiration were  $381$  and  $260 \text{ Mg yr}^{-1}$ , respectively. Combining the source and sink terms, the global forest ecosystem represents a net sink of  $\sim 1930 \text{ Mg yr}^{-1}$  of atmospheric Hg. The value is much larger than the estimate of Hg uptake by forest above-ground biomass (Obrist, 2007). The estimate by Obrist (2007) did not include deposition flux by throughfall, and the Hg concentration in biomass used in the study was 2–10 times lower than the measured Hg contents in North America, Europe, China and South America (Lindberg et al., 2007; Obrist, 2007; Risch et al., 2012; Teixeira et al., 2012; Fu et al., 2015). Our estimate is comparable to the upper limit of atmospheric Hg deposition to terrestrial ecosystems predicted by modeling studies ( $800\text{--}1900 \text{ Mg}$ ) (Mason and Sheu, 2002; Holmes et al., 2010; Driscoll et al., 2013). This implies that the forest ecosystem may be the largest sink of atmospheric Hg in the terrestrial ecosystems, whereas other terrestrial ecosystems may represent net sources.

## 5 Data availability

Requests for data sets and materials should be addressed to Xinbin Feng (fengxinbin@vip.skleg.cn) or Xuewu Fu (fuxu-ewu@mail.gyig.ac.cn).

## Information about the Supplement

Descriptions of the simulation of NBL, turbulent diffusivity and the box model are shown in the supplementary text. The location of the Mt. Changbai forest, GEM concentrations at 4 m a.g.l. in a small clearing plot and 24 and 45 m a.g.l., diurnal trends in vertical GEM gradient, soil–air GEM flux, diurnal variations of meteorological parameters, turbulent diffusivity and seasonal variations in LAI, wind speed and wind direction at the Mt. Changbai forest are shown in Figs. S1–S7. Litterfall Hg concentrations and litter mass at the Mt. Changbai forest, isotopic composition of atmospheric GEM as well as compiled litterfall and throughfall Hg deposition fluxes, and forest soil–air GEM fluxes over the global forests are shown in Tables S1–S5.

**The Supplement related to this article is available online at doi:10.5194/acp-16-12861-2016-supplement.**

*Acknowledgements.* This work was funded by the National 973 Program of China (2013CB430003), the National Science Foundation of China (41273145, 41622305 and 41473025) and Guangzhou Science and Technology Projects (2014J4100089). We acknowledge Alexandra Steffen from Environment Canada for offering the sampling instruments, Open Research Station of Changbai Mountain Forest Ecosystems, CAS for the meteorological parameters, O<sub>3</sub> concentrations, and field sampling, and Hao Xu for assistance with field sampling.

Edited by: R. Ebinghaus

Reviewed by: two anonymous referees

## References

- Amos, H. M., Jacob, D. J., Streets, D. G., and Sunderland, E. M.: Legacy impacts of all-time anthropogenic emissions on the global mercury cycle, *Global Biogeochem. Cy.*, 27, 410–421, doi:10.1002/gbc.20040, 2013.
- Baldocchi, D. and Ryu, Y.: A Synthesis of Forest Evaporation Fluxes – from Days to Years – as Measured with Eddy Covariance, in: *Forest Hydrology and Biogeochemistry*, edited by: Levia, D. F., Carlyle-Moses, D., and Tanaka, T., Ecological Studies, Springer Netherlands, 101–116, 2011.
- Bash, J. O. and Miller, D. R.: Growing season total gaseous mercury (TGM) flux measurements over an *Acer rubrum* L. stand, *Atmos. Environ.*, 43, 5953–5961, doi:10.1016/j.atmosenv.2009.08.008, 2009.
- Bishop, K. H., Lee, Y. H., Munthe, J., and Dambrine, E.: Xylem sap as a pathway for total mercury and methylmercury transport from soils to tree canopy in the boreal forest, *Biogeochemistry*, 40, 101–113, 1998.
- Biswas, A., Blum, J. D., Bergquist, B. A., Keeler, G. J., and Xie, Z. Q.: Natural mercury isotope variation in coal deposits and organic soils, *Environ. Sci. Technol.*, 42, 8303–8309, doi:10.1021/Es801444b, 2008.
- Blum, J. D. and Bergquist, B. A.: Reporting of variations in the natural isotopic composition of mercury, *Anal. Bioanal. Chem.*, 388, 353–359, doi:10.1007/s00216-007-1236-9, 2007.
- Brunke, E.-G., Labuschagne, C., Ebinghaus, R., Kock, H. H., and Slemr, F.: Gaseous elemental mercury depletion events observed at Cape Point during 2007–2008, *Atmos. Chem. Phys.*, 10, 1121–1131, doi:10.5194/acp-10-1121-2010, 2010.
- Dai, L. M., Qi, L., Wang, Q. W., Su, D. K., Yu, D. P., Wang, Y., Ye, Y. J., Jiang, S. W., and Zhao, W.: Changes in forest structure and composition on Changbai Mountain in Northeast China, *Ann. Forest Sci.*, 68, 889–897, doi:10.1007/s13595-011-0095-x, 2011.
- Demers, J. D., Blum, J. D., and Zak, D. R.: Mercury isotopes in a forested ecosystem: Implications for air–surface exchange dynamics and the global mercury cycle, *Global Biogeochem. Cy.*, 27, 222–238, doi:10.1002/Gbc.20021, 2013.
- Demers, J. D., Sherman, L. S., Blum, J. D., Marsik, F. J., and Dvonch, J. T.: Coupling atmospheric mercury isotope ratios and meteorology to identify sources of mercury impacting a coastal urban–industrial region near Pensacola, Florida, USA, *Global Biogeochem. Cy.*, 29, 1689–1705, 2015.
- Driscoll, C. T., Mason, R. P., Chan, H. M., Jacob, D. J., and Pirrone, N.: Mercury as a Global Pollutant: Sources, Pathways, and Effects, *Environ. Sci. Technol.*, 47, 4967–4983, doi:10.1021/Es305071v, 2013.
- Ebinghaus, R., Kock, H. H., Temme, C., Einax, J. W., Lowe, A. G., Richter, A., Burrows, J. P., and Schroeder, W. H.: Antarctic springtime depletion of atmospheric mercury, *Environ. Sci. Technol.*, 36, 1238–1244, doi:10.1021/Es015710z, 2002.
- Enrico, M., Le Roux, G., Maruszczak, N., Heimbürger, L. E., Claustres, A., Fu, X. W., Sun, R. Y., and Sonke, J. E.: Atmospheric Mercury Transfer to Peat Bogs Dominated by Gaseous Elemental Mercury Dry Deposition, *Environ. Sci. Technol.*, 50, 2405–2412, doi:10.1021/acs.est.5b06058, 2016.
- Erickson, J. A. and Gustin, M. S.: Foliar exchange of mercury as a function of soil and air mercury concentrations, *Sci. Total Environ.*, 324, 271–279, doi:10.1016/j.scitotenv.2003.10.034, 2004.
- Erickson, J. A., Gustin, M. S., Schorran, D. E., Johnson, D. W., Lindberg, S. E., and Coleman, J. S.: Accumulation of atmospheric mercury in forest foliage, *Atmos. Environ.*, 37, 1613–1622, 2003.
- Faïn, X., Obrist, D., Hallar, A. G., McCubbin, I., and Rahn, T.: High levels of reactive gaseous mercury observed at a high elevation research laboratory in the Rocky Mountains, *Atmos. Phys.*, 9, 8049–8060, doi:10.5194/acp-9-8049-2009, 2009.
- Finkelstein, P. L., Ellestad, T. G., Clarke, J. F., Meyers, T. P., Schwede, D. B., Hebert, E. O., and Neal, J. A.: Ozone and sulfur dioxide dry deposition to forests: Observations and model evaluation, *J. Geophys. Res.-Atmos.*, 105, 15365–15377, doi:10.1029/2000jd900185, 2000.

- Frescholtz, T. F. and Gustin, M. S.: Soil and foliar mercury emission as a function of soil concentration, *Water Air Soil Poll.*, 155, 223–237, doi:10.1023/B:Wate.0000026530.85954.3f, 2004.
- Fu, X., Maruszczak, N., Wang, X., Gheusi, F. O., and Sonke, J. E.: Isotopic Composition of Gaseous Elemental Mercury in the Free Troposphere of the Pic du Midi Observatory, France, *Environ. Sci. Technol.*, 50, 5641–5650, doi:10.1021/acs.est.6b00033, 2016a.
- Fu, X., Maruszczak, N., Heimbürger, L.-E., Sauvage, B., Gheusi, F., Prestbo, E. M., and Sonke, J. E.: Atmospheric mercury speciation dynamics at the high-altitude Pic du Midi Observatory, southern France, *Atmos. Chem. Phys.*, 16, 5623–5639, doi:10.5194/acp-16-5623-2016, 2016b.
- Fu, X. W., Feng, X., Shang, L. H., Wang, S. F., and Zhang, H.: Two years of measurements of atmospheric total gaseous mercury (TGM) at a remote site in Mt. Changbai area, Northeastern China, *Atmos. Chem. Phys.*, 12, 4215–4226, doi:10.5194/acp-12-4215-2012, 2012.
- Fu, X. W., Heimbürger, L. E., and Sonke, J. E.: Collection of atmospheric gaseous mercury for stable isotope analysis using iodine- and chlorine-impregnated activated carbon traps, *J. Anal. Atom. Spectrom.*, 29, 841–852, doi:10.1039/C3ja50356a, 2014.
- Fu, X. W., Zhang, H., Yu, B., Wang, X., Lin, C.-J., and Feng, X. B.: Observations of atmospheric mercury in China: a critical review, *Atmos. Chem. Phys.*, 15, 9455–9476, doi:10.5194/acp-15-9455-2015, 2015.
- Gratz, L. E., Keeler, G. J., Blum, J. D., and Sherman, L. S.: Isotopic composition and fractionation of mercury in Great Lakes precipitation and ambient air, *Environ. Sci. Technol.*, 44, 7764–7770, doi:10.1021/Es100383w, 2010.
- Graydon, J. A., St Louis, V. L., Lindberg, S. E., Hintelmann, H., and Krabbenhoft, D. P.: Investigation of mercury exchange between forest canopy vegetation and the atmosphere using a new dynamic chamber, *Environ. Sci. Technol.*, 40, 4680–4688, doi:10.1021/Es0604616, 2006.
- Gustin, M. and Jaffe, D.: Reducing the Uncertainty in Measurement and Understanding of Mercury in the Atmosphere, *Environ. Sci. Technol.*, 44, 2222–2227, doi:10.1021/Es902736k, 2010.
- Gustin, M. S., Ericksen, J. A., Schorran, D. E., Johnson, D. W., Lindberg, S. E., and Coleman, J. S.: Application of controlled mesocosms for understanding mercury air-soil-plant exchange, *Environ. Sci. Technol.*, 38, 6044–6050, doi:10.1021/Es0487933, 2004.
- Gustin, M. S., Huang, J. Y., Miller, M. B., Peterson, C., Jaffe, D. A., Ambrose, J., Finley, B. D., Lyman, S. N., Call, K., Talbot, R., Feddersen, D., Mao, H. T., and Lindberg, S. E.: Do we understand what the mercury speciation instruments are actually measuring? Results of RAMIX, *Environ. Sci. Technol.*, 47, 7295–7306, doi:10.1021/Es3039104, 2013.
- Gustin, M. S., Amos, H. M., Huang, J., Miller, M. B., and Heidecorn, K.: Measuring and modeling mercury in the atmosphere: a critical review, *Atmos. Chem. Phys.*, 15, 5697–5713, doi:10.5194/acp-15-5697-2015, 2015.
- Hanson, P. J., Lindberg, S. E., Tabberer, T. A., Owens, J. G., and Kim, K. H.: Foliar Exchange of Mercury-Vapor – Evidence for a Compensation Point, *Water Air Soil Poll.*, 80, 373–382, doi:10.1007/Bf01189687, 1995.
- Hedgecock, I. M. and Pirrone, N.: Chasing quicksilver: Modeling the atmospheric lifetime of  $\text{Hg}^0(\text{g})$  in the marine boundary layer at various latitudes, *Environ. Sci. Technol.*, 38, 69–76, doi:10.1021/Es034623z, 2004.
- Hens, K., Novelli, A., Martinez, M., Auld, J., Axinte, R., Bohn, B., Fischer, H., Keronen, P., Kubistin, D., Nölscher, A. C., Oswald, R., Paasonen, P., Petäjä, T., Regelin, E., Sander, R., Sinha, V., Sipilä, M., Taraborrelli, D., Tatum Ernest, C., Williams, J., Lelieveld, J., and Harder, H.: Observation and modelling of  $\text{HO}_x$  radicals in a boreal forest, *Atmos. Chem. Phys.*, 14, 8723–8747, doi:10.5194/acp-14-8723-2014, 2014.
- Holmes, C. D., Jacob, D. J., and Yang, X.: Global lifetime of elemental mercury against oxidation by atomic bromine in the free troposphere, *Geophys. Res. Lett.*, 33, L20808, doi:10.1029/2006gl027176, 2006.
- Holmes, C. D., Jacob, D. J., Corbitt, E. S., Mao, J., Yang, X., Talbot, R., and Slemr, F.: Global atmospheric model for mercury including oxidation by bromine atoms, *Atmos. Chem. Phys.*, 10, 12037–12057, doi:10.5194/acp-10-12037-2010, 2010.
- Huang, J. Y. and Gustin, M. S.: Use of Passive Sampling Methods and Models to Understand Sources of Mercury Deposition to High Elevation Sites in the Western United States, *Environ. Sci. Technol.*, 49, 432–441, doi:10.1021/es502836w, 2015.
- Huang, J. Y., Miller, M. B., Weiss-Penzias, P., and Gustin, M. S.: Comparison of gaseous oxidized Hg measured by KCl-coated denuders, and Nylon and Cation exchange Membranes, *Environ. Sci. Technol.*, 47, 7307–7316, doi:10.1021/Es4012349, 2013.
- Kim, K. H., Lindberg, S. E., and Meyers, T. P.: Micrometeorological Measurements of Mercury-Vapor Fluxes over Background Forest Soils in Eastern Tennessee, *Atmos. Environ.*, 29, 267–282, doi:10.1016/1352-2310(94)00198-T, 1995.
- Lan, X., Talbot, R., Castro, M., Perry, K., and Luke, W.: Seasonal and diurnal variations of atmospheric mercury across the US determined from AMNet monitoring data, *Atmos. Chem. Phys.*, 12, 10569–10582, doi:10.5194/acp-12-10569-2012, 2012.
- Landis, M. S., Stevens, R. K., Schaedlich, F., and Prestbo, E. M.: Development and characterization of an annular denuder methodology for the measurement of divalent inorganic reactive gaseous mercury in ambient air, *Environ. Sci. Technol.*, 36, 3000–3009, doi:10.1021/Es015887t, 2002.
- Lindberg, S., Bullock, R., Ebinghaus, R., Engstrom, D., Feng, X. B., Fitzgerald, W., Pirrone, N., Prestbo, E., and Seigneur, C.: A synthesis of progress and uncertainties in attributing the sources of mercury in deposition, *Ambio*, 36, 19–32, 2007.
- Lindberg, S. E. and Stratton, W. J.: Atmospheric mercury speciation: Concentrations and behavior of reactive gaseous mercury in ambient air, *Environ. Sci. Technol.*, 32, 49–57, doi:10.1021/es970546u, 1998.
- Lindberg, S. E., Hanson, P. J., Meyers, T. P., and Kim, K. H.: Air/surface exchange of mercury vapor over forests - The need for a reassessment of continental biogenic emissions, *Atmos. Environ.*, 32, 895–908, doi:10.1016/S1352-2310(97)00173-8, 1998.
- Lindberg, S. E., Brooks, S., Lin, C. J., Scott, K. J., Landis, M. S., Stevens, R. K., Goodsite, M., and Richter, A.: Dynamic oxidation of gaseous mercury in the Arctic troposphere at polar sunrise, *Environ. Sci. Technol.*, 36, 1245–1256, doi:10.1021/Es0111941, 2002.
- Lyman, S. N. and Jaffe, D. A.: Formation and fate of oxidized mercury in the upper troposphere and lower stratosphere, *Nat. Geosci.*, 5, 114–117, doi:10.1038/Ngeo1353, 2012.

- Mao, H., Talbot, R. W., Sigler, J. M., Sive, B. C., and Hegarty, J. D.: Seasonal and diurnal variations of Hg<sup>0</sup> over New England, *Atmos. Chem. Phys.*, 8, 1403–1421, doi:10.5194/acp-8-1403-2008, 2008.
- Mason, R. P. and Sheu, G. R.: Role of the ocean in the global mercury cycle, *Global Biogeochem. Cy.*, 16, 1093, doi:10.1029/2001gb001440, 2002.
- Millhollen, A. G., Gustin, M. S., and Obrist, D.: Foliar mercury accumulation and exchange for three tree species, *Environ. Sci. Technol.*, 40, 6001–6006, doi:10.1021/Es0609194, 2006.
- Munger, J. W., Wofsy, S. C., Bakwin, P. S., Fan, S. M., Goulden, M. L., Daube, B. C., Goldstein, A. H., Moore, K. E., and Fitzjarrald, D. R.: Atmospheric deposition of reactive nitrogen oxides and ozone in a temperate deciduous forest and a subarctic woodland. I. Measurements and mechanisms, *J. Geophys. Res.-Atmos.*, 101, 12639–12657, doi:10.1029/96jd00230, 1996.
- Obrist, D.: Atmospheric mercury pollution due to losses of terrestrial carbon pools?, *Biogeochemistry*, 85, 119–123, doi:10.1007/s10533-007-9108-0, 2007.
- Obrist, D., Tas, E., Peleg, M., Matveev, V., Fain, X., Asaf, D., and Luria, M.: Bromine-induced oxidation of mercury in the mid-latitude atmosphere, *Nat. Geosci.*, 4, 22–26, doi:10.1038/Ngeo1018, 2011.
- Pan, Y. D., Birdsey, R. A., Fang, J. Y., Houghton, R., Kauppi, P. E., Kurz, W. A., Phillips, O. L., Shvidenko, A., Lewis, S. L., Canadell, J. G., Ciais, P., Jackson, R. B., Pacala, S. W., McGuire, A. D., Piao, S. L., Rautiainen, A., Sitch, S., and Hayes, D.: A Large and Persistent Carbon Sink in the World's Forests, *Science*, 333, 988–993, doi:10.1126/science.1201609, 2011.
- Poissant, L., Pilote, M., Yumvihoze, E., and Lean, D.: Mercury concentrations and foliage/atmosphere fluxes in a maple forest ecosystem in Quebec, Canada, *J. Geophys. Res.-Atmos.*, 113, D10307, doi:10.1029/2007jd009510, 2008.
- Rea, A. W., Lindberg, S. E., and Keeler, G. J.: Assessment of dry deposition and foliar leaching of mercury and selected trace elements based on washed foliar and surrogate surfaces, *Environ. Sci. Technol.*, 34, 2418–2425, doi:10.1021/es991305k, 2000.
- Rinne, J., Markkanen, T., Ruuskanen, T. M., Petäjä, T., Keronen, P., Tang, M. J., Crowley, J. N., Rannik, Ü., and Vesala, T.: Effect of chemical degradation on fluxes of reactive compounds – a study with a stochastic Lagrangian transport model, *Atmos. Chem. Phys.*, 12, 4843–4854, doi:10.5194/acp-12-4843-2012, 2012.
- Risch, M. R., DeWild, J. F., Krabbenhoft, D. P., Kolka, R. K., and Zhang, L. M.: Litterfall mercury dry deposition in the eastern USA, *Environ. Pollut.*, 161, 284–290, doi:10.1016/j.envpol.2011.06.005, 2012.
- Schroeder, W. H., Anlauf, K. G., Barrie, L. A., Lu, J. Y., Steffen, A., Schneeberger, D. R., and Berg, T.: Arctic springtime depletion of mercury, *Nature*, 394, 331–332, doi:10.1038/28530, 1998.
- Selin, N. E., Jacob, D. J., Park, R. J., Yantosca, R. M., Strode, S., Jaegle, L., and Jaffe, D.: Chemical cycling and deposition of atmospheric mercury: Global constraints from observations, *J. Geophys. Res.-Atmos.*, 112, D02308, doi:10.1029/2006jd007450, 2007.
- Selin, N. E., Jacob, D. J., Yantosca, R. M., Strode, S., Jaegle, L., and Sunderland, E. M.: Global 3-D land-ocean-atmosphere model for mercury: Present-day versus preindustrial cycles and anthropogenic enrichment factors for deposition, *Global Biogeochem. Cy.*, 22, Gb2011, doi:10.1029/2007gb003040, 2008.
- Shah, V., Jaegle, L., Gratz, L. E., Ambrose, J. L., Jaffe, D. A., Selin, N. E., Song, S., Campos, T. L., Flocke, F. M., Reeves, M., Stechman, D., Stell, M., Festa, J., Stutz, J., Weinheimer, A. J., Knapp, D. J., Montzka, D. D., Tyndall, G. S., Apel, E. C., Hornbrook, R. S., Hills, A. J., Riemer, D. D., Blake, N. J., Cantrell, C. A., and Mauldin III, R. L.: Origin of oxidized mercury in the summertime free troposphere over the southeastern US, *Atmos. Chem. Phys.*, 16, 1511–1530, doi:10.5194/acp-16-1511-2016, 2016.
- Sherman, L. S., Blum, J. D., Johnson, K. P., Keeler, G. J., Barres, J. A., and Douglas, T. A.: Mass-independent fractionation of mercury isotopes in Arctic snow driven by sunlight, *Nat. Geosci.*, 3, 173–177, doi:10.1038/Ngeo758, 2010.
- Sheu, G. R., Lin, N. H., Wang, J. L., Lee, C. T., Yang, C. F. O., and Wang, S. H.: Temporal distribution and potential sources of atmospheric mercury measured at a high-elevation background station in Taiwan, *Atmos. Environ.*, 44, 2393–2400, doi:10.1016/j.atmosenv.2010.04.009, 2010.
- Shi, T. T., Guan, D. X., Wang, A. Z., Wu, J. B., Jin, C. J., and Han, S. J.: Comparison of three models to estimate evapotranspiration for a temperate mixed forest, *Hydrol. Process.*, 22, 3431–3443, doi:10.1002/hyp.6922, 2008.
- Slemr, F., Ebinghaus, R., Brenninkmeijer, C. A. M., Hermann, M., Kock, H. H., Martinsson, B. G., Schuck, T., Sprung, D., van Velthoven, P., Zahn, A., and Ziereis, H.: Gaseous mercury distribution in the upper troposphere and lower stratosphere observed onboard the CARIBIC passenger aircraft, *Atmos. Chem. Phys.*, 9, 1957–1969, doi:10.5194/acp-9-1957-2009, 2009.
- Sommar, J., Zhu, W., Lin, C. J., and Feng, X. B.: Field Approaches to Measure Hg Exchange Between Natural Surfaces and the Atmosphere A Review, *Crit. Rev. Env. Sci. Tec.*, 43, 1657–1739, doi:10.1080/10643389.2012.671733, 2013.
- Sonke, J. E. and Fu, X. W.: Mass dependent and independent fractionation of mercury isotopes during tropospheric elemental mercury transformations, in preparation, 2016.
- Spivakovsky, C. M., Logan, J. A., Montzka, S. A., Balkanski, Y. J., Foreman-Fowler, M., Jones, D. B. A., Horowitz, L. W., Fusco, A. C., Brenninkmeijer, C. A. M., Prather, M. J., Wofsy, S. C., and McElroy, M. B.: Three-dimensional climatological distribution of tropospheric OH: Update and evaluation, *J. Geophys. Res.-Atmos.*, 105, 8931–8980, doi:10.1029/1999jd901006, 2000.
- Stamenkovic, J. and Gustin, M. S.: Nonstomatal versus Stomatal Uptake of Atmospheric Mercury, *Environ. Sci. Technol.*, 43, 1367–1372, doi:10.1021/Es801583a, 2009.
- Stathopoulos, D.: Fractionation of mercury isotopes in an aqueous environment: Chemical Oxidation, Master Dissertation, Trent University, Peterborough, Ontario, Canada, 2014.
- Steffen, A., Douglas, T., Amyot, M., Ariya, P., Aspino, K., Berg, T., Bottenheim, J., Brooks, S., Cobbett, F., Dastoor, A., Dommergue, A., Ebinghaus, R., Ferrari, C., Gardfeldt, K., Goodsite, M. E., Lean, D., Poulain, A. J., Scherz, C., Skov, H., Sommar, J., and Temme, C.: A synthesis of atmospheric mercury depletion event chemistry in the atmosphere and snow, *Atmos. Chem. Phys.*, 8, 1445–1482, doi:10.5194/acp-8-1445-2008, 2008.
- Strode, S. A., Jaegle, L., Selin, N. E., Jacob, D. J., Park, R. J., Yantosca, R. M., Mason, R. P., and Slemr, F.: Air-sea exchange in the global mercury cycle, *Global Biogeochem. Cy.*, 21, Gb1017, doi:10.1029/2006gb002766, 2007.
- Sun, G., Sommar, J., Feng, X., Lin, C.-J., Ge, M., Wang, W., Yin, R., Fu, X., and Shang, L.: Mass-dependent and -independent frac-

- tionation of mercury isotope during gas-phase oxidation of elemental mercury vapor by atomic Cl and Br, *Environ. Sci. Technol.*, 50, 9232–9241, doi:10.1021/acs.est.6b01668, 2016.
- Sun, R. Y., Enrico, M., Heimburger, L. E., Scott, C., and Sonke, J. E.: A double-stage tube furnace-acid-trapping protocol for the pre-concentration of mercury from solid samples for isotopic analysis, *Anal. Bioanal. Chem.*, 405, 6771–6781, doi:10.1007/s00216-013-7152-2, 2013.
- Swartzendruber, P. C., Jaffe, D. A., Prestbo, E. M., Weiss-Penzias, P., Selin, N. E., Park, R., Jacob, D. J., Strode, S., and Jaegle, L.: Observations of reactive gaseous mercury in the free troposphere at the Mount Bachelor Observatory, *J. Geophys. Res.-Atmos.*, 111, D24301, doi:10.1029/2006jd007415, 2006.
- Swartzendruber, P. C., Jaffe, D. A., and Finley, B.: Improved fluorescence peak integration in the Tekran 2537 for applications with sub-optimal sample loadings, *Atmos. Environ.*, 43, 3648–3651, doi:10.1016/j.atmosenv.2009.02.063, 2009a.
- Swartzendruber, P. C., Jaffe, D. A., and Finley, B.: Development and First Results of an Aircraft-Based, High Time Resolution Technique for Gaseous Elemental and Reactive (Oxidized) Gaseous Mercury, *Environ. Sci. Technol.*, 43, 7484–7489, doi:10.1021/Es901390t, 2009b.
- Talbot, R., Mao, H. T., and Sive, B.: Diurnal characteristics of surface level O<sub>3</sub> and other important trace gases in New England, *J. Geophys. Res.-Atmos.*, 110, D09307, doi:10.1029/2004JD005449, 2005.
- Teixeira, D. C., Montezuma, R. C., Oliveira, R. R., and Silva, E. V.: Litterfall mercury deposition in Atlantic forest ecosystem from SE – Brazil, *Environ. Pollut.*, 164, 11–15, doi:10.1016/j.envpol.2011.10.032, 2012.
- Timonen, H., Ambrose, J. L., and Jaffe, D. A.: Oxidation of elemental Hg in anthropogenic and marine airmasses, *Atmos. Chem. Phys.*, 13, 2827–2836, doi:10.5194/acp-13-2827-2013, 2013.
- Yang, X., Cox, R. A., Warwick, N. J., Pyle, J. A., Carver, G. D., O'Connor, F. M., and Savage, N. H.: Tropospheric bromine chemistry and its impacts on ozone: A model study, *J. Geophys. Res.-Atmos.*, 110, D23311, doi:10.1029/2005jd006244, 2005.
- Yin, R. S., Feng, X. B., and Meng, B.: Stable Mercury Isotope Variation in Rice Plants (*Oryza sativa* L.) from the Wanshan Mercury Mining District, SW China, *Environ. Sci. Technol.*, 47, 2238–2245, doi:10.1021/Es304302a, 2013.
- Zhang, H. H., Poissant, L., Xu, X. H., and Pilote, M.: Explorative and innovative dynamic flux bag method development and testing for mercury air-vegetation gas exchange fluxes, *Atmos. Environ.*, 39, 7481–7493, doi:10.1016/j.atmosenv.2005.07.068, 2005.
- Zhang, L., Blanchard, P., Gay, D. A., Prestbo, E. M., Risch, M. R., Johnson, D., Narayan, J., Zsolway, R., Holsen, T. M., Miller, E. K., Castro, M. S., Graydon, J. A., Louis, V. L. St., and Dalziel, J.: Estimation of speciated and total mercury dry deposition at monitoring locations in eastern and central North America, *Atmos. Chem. Phys.*, 12, 4327–4340, doi:10.5194/acp-12-4327-2012, 2012.
- Zhang, L. M., Gong, S. L., Padro, J., and Barrie, L.: A size-segregated particle dry deposition scheme for an atmospheric aerosol module, *Atmos. Environ.*, 35, 549–560, doi:10.1016/S1352-2310(00)00326-5, 2001.
- Zhang, L. M., Wright, L. P., and Blanchard, P.: A review of current knowledge concerning dry deposition of atmospheric mercury, *Atmos. Environ.*, 43, 5853–5864, doi:10.1016/j.atmosenv.2009.08.019, 2009.
- Zhou, Y., Su, J. Q., Janssens, I. A., Zhou, G. S., and Xiao, C. W.: Fine root and litterfall dynamics of three Korean pine (*Pinus koraiensis*) forests along an altitudinal gradient, *Plant Soil*, 374, 19–32, doi:10.1007/s11104-013-1816-8, 2014.